

Low-energy subgap states in multichannel p -wave superconducting wires

G. Kells, D. Meidan, and P. W. Brouwer

Dahlem Center for Complex Quantum Systems and Fachbereich Physik, Freie Universität Berlin, Arnimallee 14, 14195 Berlin, Germany

(Received 21 October 2011; revised manuscript received 13 January 2012; published 29 February 2012)

One-dimensional p -wave superconductors are known to harbor Majorana bound states at their ends. Superconducting wires with a finite width W may have fermionic subgap states in addition to possible Majorana end states. While they do not necessarily inhibit the use of Majorana end states for topological computation, these subgap states can obscure the identification of a topological phase through a density-of-states measurement. We present two simple models to describe low-energy fermionic subgap states. If the wire's width W is much smaller than the superconductor coherence length ξ , the relevant subgap states are localized near the ends of the wire and cluster near zero energy, whereas the lowest-energy subgap states are delocalized if $W \gtrsim \xi$. Notably, the energy of the lowest-lying fermionic subgap state (if present at all) has a maximum for $W \sim \xi$.

DOI: [10.1103/PhysRevB.85.060507](https://doi.org/10.1103/PhysRevB.85.060507)

PACS number(s): 74.78.Na, 74.20.Rp, 03.67.Lx, 73.63.Nm

The search for Majorana fermions has attracted a great deal of interest in the past few years.¹ Notably their nonlocal properties and non-Abelian braiding statistics make Majorana fermion systems attractive candidates for fault-tolerant quantum computation.^{2–5} The present wave of interest is driven by a number of proposals that suggest ways of realizing and manipulating Majorana states in solid-state systems, most prominently interfaces of s -wave superconductors and topological insulators,^{6,7} half-metallic ferromagnets,^{8–10} or semiconductor films or wires,^{11,12} where the latter stand out because Majorana manipulation requires a mere series of gate operations.¹³ In all these proposals, the underlying principle is that with the right conditions the proximity coupling to the s -wave superconductor can turn the wire material into a p -wave superconductor. These p -wave superconductors are predicted to support Majorana fermions at their ends, edges, or along domain walls separating different topological phases.^{14–17}

Majorana bound states at ends of what is effectively a p -wave superconducting wire can be analyzed most straightforwardly if these wires are strictly one dimensional, with only a single propagating mode at the Fermi level in the absence of superconductivity.^{11,12} Nevertheless, Majorana end states can also exist in a quasi-one-dimensional geometry. The effect of multiple transverse channels, present in most realistic realizations, has been addressed in Refs. 18–23. Specifically one sees that a complex p -wave superconductor in a strip geometry undergoes a series of oscillatory quantum phase transitions between topologically trivial and topologically nontrivial phases (without and with Majorana end states, respectively) as the strip width W or chemical potential μ are varied. Both with and without Majorana end states, a range of subgap states is found,¹⁹ analogous to the subgap states in vortex cores of bulk superconductors.^{24,25} Although the mere presence of subgap states does not prohibit the use of Majorana end states for topological quantum computation,²⁶ the presence of low-lying subgap states clearly obstructs an unambiguous experimental verification of the Majorana states.

The purpose of this Rapid Communication is to systematically analyze the energies of the subgap states as a function of the sample width W . Throughout we assume that $\xi \gtrsim \lambda_F$, where $\lambda_F = 2\pi/k_F$ is the Fermi wavelength in

the absence of superconductivity and ξ the superconducting coherence length. Our results, which will be discussed in detail below, reveal two different regimes, depending on the relative magnitude of W and ξ :

(1) If $W \lesssim \xi$ there is an alternation of topological and nontopological phases, where each phase harbors at most one Majorana state at zero energy and $N_f \leq N = \text{int}[(W/\pi)\sqrt{k_F^2 - \xi^{-2}}]$ fermionic subgap states localized near each end of the wire (see Fig. 1). The lowest-lying fermionic subgap state (if present) has energy

$$\varepsilon_{\min} \sim \Delta \frac{W\lambda_F}{\xi^2 \ln(W/\lambda_F)}. \quad (1)$$

For wire widths $W \ll \xi^{2/3}\lambda_F^{1/3}$ one has $N_f = N$ and the highest-lying subgap state has energy $\sim \Delta W^3/\xi^2\lambda_F$, well below the bulk excitation gap Δ .

(2) For $W \gtrsim \xi$ there is an alternation of topological and nontopological phases, with Majorana end states in the topological phase, and delocalized subgap states with minimum energy

$$\varepsilon_{\min} \sim \Delta e^{-W/\xi}. \quad (2)$$

Equation (2) was obtained previously in Ref. 23.

We note that as most experimental proposals involve a rather weak induced superconductivity because of the presence of Schottky barrier or the dependence on spin-orbit coupling, we believe that the quasi-one-dimensional regime $W/\xi \ll 1$ is most relevant for possible applications. Hence, these findings imply that, in the experimentally accessible regime, localized subgap states cluster around zero energy, thus obstructing the experimental verification of Majorana states through a density-of-states measurement (see Fig. 1). In fact, the optimal wire width W that gives rise to the largest excitation gap to fermionic subgap states is $W \sim \xi$ (Fig. 2), although the optimal excitation gap for a multichannel wire is always lower than that of a single-channel wire. Nonetheless, for $W/\xi \ll 1$ there is no coupling between subgap states localized at opposite ends of the strip, as the excitation gap to delocalized bulk states is large ($\gtrsim \Delta$; see Fig. 1), making the narrow limit favorable for topological protection. Our analysis provides a straightforward physical interpretation of the oscillatory quantum phase transitions and highlights broad

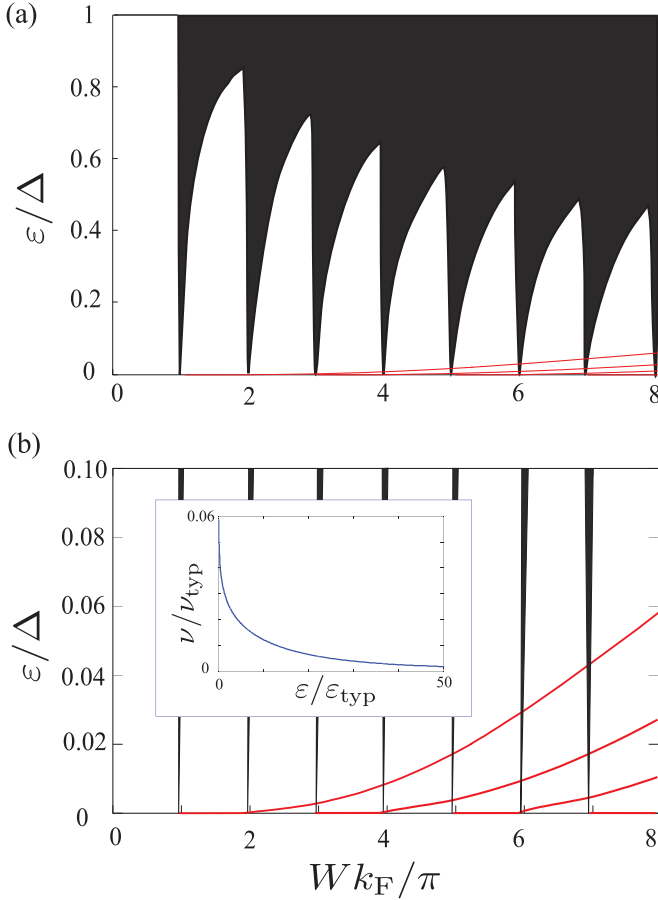


FIG. 1. (Color online) (a) Excitation spectrum of a p -wave superconducting strip as a function of the strip width W , for small Wk_F . The solid (red) curves and the shaded region indicate the discrete energies of the end states and the continuous spectrum, respectively. The data shown in the figure is obtained from a solution of the effective models described in the text with $k_F\xi = 100$. Data points obtained from a numerical solution of the lattice with $-4t < \mu < -3t$ were used to generate this plot. (b) Closeup of x axis of (a). In the inset we show the density of fermionic end states in the limit $\lambda_F \ll W \ll \xi$. Here $\epsilon_{\text{typ}} = \pi \Delta (W/\xi)^2$ and $\nu_{\text{typ}} = Wk_F/(\pi \epsilon_{\text{typ}})$.

similarities between the \mathbb{Z} -to- \mathbb{Z}_2 crossover and the nucleation of topological phases discussed, for example, in Refs. 27 and 28.

For the detailed discussion of these findings we employ a two-dimensional lattice model of a complex p -wave superconductor.^{15,17,29} The same model was studied recently in Refs. 18,19,30, and 31. We consider a strip geometry of length $L = N_x a$ and width $W = N_y a$, where a is the lattice constant, with the Hamiltonian

$$\begin{aligned}
 H = & -\mu \sum_{i=1}^{N_x} \sum_{j=1}^{N_y} c_{i,j}^\dagger c_{i,j} \\
 & - \sum_{i=1}^{N_x-1} \sum_{j=1}^{N_y} (t c_{i+1,j}^\dagger c_{i,j} - i \Delta_x c_{i+1,j}^\dagger c_{i,j}^\dagger + \text{H.c.}) \\
 & - \sum_{i=1}^{N_x} \sum_{j=1}^{N_y-1} (t c_{i,j+1}^\dagger c_{i,j} + \Delta_y c_{i,j+1}^\dagger c_{i,j}^\dagger + \text{H.c.}), \quad (3)
 \end{aligned}$$

where μ is the chemical potential, t the hopping amplitude, and Δ_x and Δ_y set the p -wave pairing amplitudes in the longitudinal and transverse directions, respectively. We will focus on the scenario that the p -wave superconducting order is inherited from proximity coupling to a bulk superconductor, as in the proposals of Refs. 6–12 and 20, so that no self-consistency conditions need to be accounted for. The bulk dispersion of Eq. (3) gives excitations at energies

$$\begin{aligned}
 E_k^2 = & [-\mu - 2t(\cos k_x a + \cos k_y a)]^2 \\
 & + 4\Delta_x^2 \sin^2 k_x a + 4\Delta_y^2 \sin^2 k_y a. \quad (4)
 \end{aligned}$$

Below we will set $\Delta_x = \Delta_y$ and formulate our main results in the continuum limit, which is obtained by sending $a \rightarrow 0$ while keeping L , W , and the number of electrons fixed. In this limit, $\mu \rightarrow -4t + t(k_F a)^2$ and $E_k \rightarrow k_F^{-1} \sqrt{(k^2 - k_F^2)^2 (\hbar v_F)^2 + k^2 \Delta^2}$, where $k_F = 2\pi/\lambda_F$ is the Fermi wave number, $\hbar v_F = 2tk_F a^2$ the Fermi velocity, and $\Delta = 2\Delta_x k_F a = 2\Delta_y k_F a$ the bulk excitation gap. The superconductor coherence length is $\xi = \hbar v_F/\Delta$. The model (3) falls into class D in the symmetry classification of noninteracting topological insulators and superconductors.^{32,33} In one dimension, the archetypal model in the D class is the so-called Majorana chain or wire,¹⁵ which is characterized by a \mathbb{Z}_2 topological invariant. In the two-dimensional (2D) limit, class D is characterized by a \mathbb{Z} topological invariant. This model, and its $k_x - ik_y$ partner, correspond to realizations with Chern numbers of $\sigma = 0, \pm 1$; examples of higher Chern numbers do exist (see e.g., Refs. 16 and 34–36).

For $W < \pi(k_F^2 - \xi^2)^{-1/2}$ the model (3) is a trivial insulator. Upon increasing the sample width, the system undergoes a series of topological phase transitions. In order to study low-lying excitations in each phase, we use two separate calculations, valid for $W \ll \xi$ and $W \gtrsim \xi$, respectively.

The case $W \ll \xi$. If $W \ll \xi$, hypothetical end states have a vanishing expectation value of the transverse momentum p_y . For this reason, it is a good approximation to treat the term proportional to Δ_y in the Hamiltonian (3) in perturbation theory. Solving for the eigenstates of Eq. (3) with $\Delta_y = 0$ in the limit of large L , we find (in the continuum limit)

$$N = \text{int}[(W/\pi)\sqrt{k_F^2 - \xi^{-2}}], \quad (5)$$

zero-energy Majorana states at the left (+) or right (−) ends of the wire, with annihilation/creation operators $\gamma_{n,\pm} = e^{\mp i\pi/4} \sum_{i,j} u_{n,\pm}(ia, ja)(c_{i,j} \pm i c_{i,j}^\dagger)$, $n = 1, 2, \dots, N$, and

$$u_{n,+}(x, y) = \sqrt{\frac{2}{W}} \Omega_n^{-1/2} \sin(n\pi y/W) \sin(k_{nx} x) e^{-x/\xi}. \quad (6)$$

Here $k_{nx}^2 = k_F^2 - (n\pi/W)^2 - \xi^{-2}$, Ω_n is a normalization constant, and $u_{n,-}(x, y) = u_{n,+}(L - x, y)$. Full results for the lattice model are qualitatively similar (see Refs. 4,16,23, and 37–39). The pairing term proportional to Δ_y is then treated in degenerate perturbation theory. Using the N zero-energy

states of Eq. (6) at each end as a basis, one finds the effective $N \times N$ Hamiltonian H_{nm} with $H_{nm} = 0$ if $n + m$ is even and

$$H_{nm} = \frac{32i \Delta \lambda_F m n}{\pi W(m^2 - n^2)} \times \frac{\sqrt{(4W^2 - \lambda_F^2 n^2)(4W^2 - \lambda_F^2 m^2)}}{(8W)^2 - 8\lambda_F^2(n^2 + m^2) + \frac{\lambda_F^2 \xi^2}{W^2}(n^2 - m^2)^2} \quad (7)$$

if $n + m$ is odd. The eigenvalues ε of the antisymmetric matrix (7) come in pairs $\pm\varepsilon$; the Hamiltonian (7) has a single zero eigenvalue if N is odd. In that case the corresponding zero mode at the left or right end is a linear combination of orbitals $u_{n,\pm}(x, y)$ with n odd only. The topologically trivial phases, which have no zero-energy end states, occur for even N . Since N increases stepwise as the chemical potential μ or the width W is varied, the system thus undergoes a sequence of topological phase transitions. We could not obtain a closed-form expression for the eigenvalues of the effective Hamiltonian (7) for general N . A simple scaling analysis of the Hamiltonian (7) shows that the lowest positive eigenvalue ε_{\min} is of order $\Delta \lambda_F \min(W/\xi^2, 1/W)$, so that the optimal (largest) separation between the Majorana state and the lowest-lying fermionic excitation is achieved for W of order ξ . A numerical evaluation of the spectrum reveals an additional logarithmic correction in the limit $W \ll \xi$, thus giving the estimate (1) for $W \ll \xi$. The highest eigenvalue of the matrix (7) is of order $\Delta \max(1, W^3/\lambda_F \xi^2)$. For $W \lesssim \xi$, the density of states has median $\varepsilon_{\text{typ}} \sim \pi \Delta(W/\xi)^2$, well below the bulk excitation gap Δ , thus justifying the perturbative procedure [see Fig. 1 (inset)].

For $W \sim \xi$, the spectrum of end states found here is similar to that of the subgap states in a vortex core,²⁴ which appear at a regular spacing $\sim \Delta \lambda_F/\xi$, filling up the entire region between zero excitation energy and the bulk gap Δ . On the other hand, in the limit that the wire width is small in comparison to the coherence length, the end states cluster near zero excitation energy and their spacing is anomalously small.

The case $W \gtrsim \xi$. The end states discussed so far are not the only possible low-energy excitations of the system. In addition to the end states, there are lateral Majorana modes localized near the edges at $y = 0$ and $y = W$.^{14,16} At transition points between the topological phases, the lowest energies of these lateral edge modes drops to zero [see the discussion below Eq. (8) for details], so that the effective Hamiltonian (7) provides a complete description of the low-energy excitations away from the transition points only. Moreover, away from the transition points, the energy splitting of the lateral modes decreases exponentially as the width increases, and eventually they become the dominant low-energy excitation for sufficiently large $W \gtrsim \xi$, with an excitation gap that follows $\sim \Delta e^{-W/\xi}$.

In order to gain a deeper understanding of the role of the lateral Majorana modes, we now apply periodic boundary conditions in the longitudinal (x) direction, while keeping the hard boundaries at $y = 0$ (+) and $y = W$ (-). The calculation presented here allows one to calculate the excitation gap to the lateral edge modes in the continuum limit and reveals that the \mathbb{Z}_2 topological order of the bulk can be understood as an effective Majorana hopping model. The Majorana modes

on the lateral edges are labeled by the wave number k_x and have operators $\gamma_{k_x, \pm} = \sum_{m,n} u_{k_x, \pm}(na) e^{ik_x ma} (c_{m,n} \pm c_{m,n}^\dagger)$ and energy $\varepsilon_{\pm}(k_x)$. In the limit $W/\xi \rightarrow \infty$ the wave functions $u_{k_x, \pm}(y)$ are known,^{16,38,39}

$$u_{k_x, +}(y) = \frac{e^{-y/\xi} \sin(k_y y)}{\sqrt{\Omega_{k_x}}}, \quad k_y = \sqrt{k_F^2 - k_x^2 - \xi^{-2}}, \quad (8)$$

with Ω_{k_x} a normalization constant and $u_{k_x, -}(y) = i u_{k_x, +}(W - y)$, and their energy is

$$\varepsilon_{\pm}(k_x) = \pm \xi(k_x), \quad \xi(k_x) = k_x \Delta / k_F. \quad (9)$$

The wave functions (8) also satisfy the boundary conditions for finite W if $k_y W/\pi$ is an integer. These special points, at which the spectrum of the lateral Majorana modes is gapless, correspond to the boundaries between the topological and nontopological phases.²³ [Note the consistency with Eq. (5) above.] In the vicinity of the phase boundary at $k_y = k_y^c = m_y \pi / W$, m_y integer, the energies of the lateral Majorana modes can be obtained in perturbation theory, which leads to the effective 2×2 matrix Hamiltonian

$$H_{k_x} = \begin{pmatrix} \xi(k_x) & h(k_x) \\ h(k_x) & -\xi(k_x) \end{pmatrix}, \quad (10)$$

for the lateral Majorana modes, with

$$h(k_x) = -i \frac{\hbar v_F}{2k_F} [(k_y^c)^2 - k_y^2] \langle u_{k_x, +}^c | u_{k_x, -}^c \rangle, \quad (11)$$

where the superscript ‘‘c’’ refers to the wave functions at the transition point, i.e., with $k_y = k_y^c$. The eigenvalues of H_{k_x} are $\varepsilon_{\pm}(k_x) = \pm [h(k_x)^2 + \xi(k_x)^2]^{1/2}$. Interestingly, the sign of $h(k_x)$ encodes the sign of the effective mass of the system¹⁴ and therefore also encodes the \mathbb{Z}_2 topological index of the system.^{15,16} Although the effective Hamiltonian (10) has been derived in the vicinity of transition points between topological and nontopological phases ($|k_y - k_y^c|$ small), comparison with a full numerical solution of the lattice model (3) shows good agreement for all W if m_y is taken to be the integer closest to $k_y W/\pi$ (agreement within 13% for $W \gg \xi$ —data not shown). Making use of the estimate $\langle u_{k_x, +}^c | u_{k_x, -}^c \rangle \approx (-1)^{m+1} (W/2\xi) e^{-W/\xi}$ for $W \gtrsim \xi$, we find that the typical gap ε_{\min} of the lateral Majorana modes away from the transition points is given by Eq. (2) if $W \gg \xi$.

Figure 2 shows the value of the energy ε_{\min} of the lowest-lying fermionic excitation at the midpoint of each topological phase, as a function of the width W . We observe that the two calculations outlined above are in excellent agreement with the full numerical calculation in the limits $W \ll \xi$ and $W \gg \xi$. Although there are quantitative deviations in the crossover between these two limits, ε_{\min} is qualitatively well described by the minimum of the two asymptotic expressions (2) and (1).

Conclusion and perspective. We have presented two simple analytical models to describe two types of low-lying fermionic excitations in a multichannel p -wave superconducting wire. The first model describes fermionic end states, which are the lowest relevant excitations for wire widths W well below the superconductor coherence length ξ . The second model applies to delocalized excitations along the wire’s edges, which are the relevant low-energy excitations if $W \gtrsim \xi$. While our

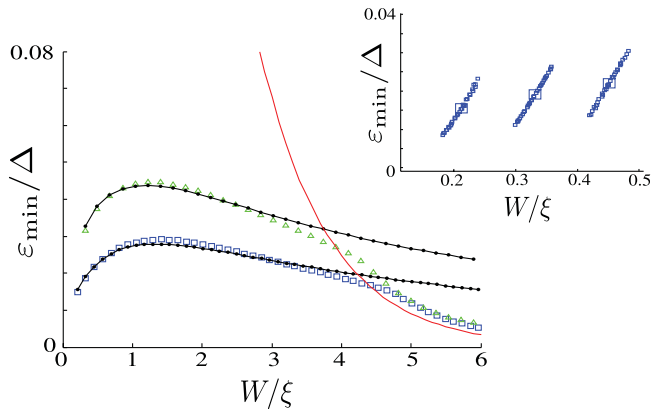


FIG. 2. (Color online) The energy ε_{\min} of the lowest-lying fermionic excitation in the topological nontrivial phases, as a function of the sample width W . The main panel shows the value of ε_{\min} at the midpoint of each topological nontrivial phase for $\mu = -3t$ (see the inset), which illustrates the large-scale dependence of ε_{\min} on the sample width W . Squares and triangles refer to full numerical solutions of the lattice model (3) for $k_F\xi = 50$ and $33\frac{1}{3}$, respectively; The dotted solid black curves and the red solid curve represent solutions of the effective models (7) and (10), respectively. Inset: ε_{\min} vs W for the topologically nontrivial phases for $k_F\xi = 50$, obtained by combining data from a numerical solution of the lattice model (3) for various values of μ near $-3t$.

results were obtained for a simplified model of a $p + ip$ superconductor, we expect that the general scaling properties presented here will remain present in a more realistic treatment of spin-orbit-coupled superconductors.

The fermionic end states, which are the relevant low-energy excitations for $W \lesssim \xi$, appear in the topological as well as in the nontopological regimes, as soon as the wire has more than one channel, $W > \pi(k_F^2 - \xi^{-2})^{-1/2}$. For thin wires, $W \ll \xi$, the fermionic end states cluster around zero energy (see Fig. 1), so that the mere observation of a large local density of states near zero energy at the end of the wire is not a reliable signature of a Majorana bound state. Energy differences of order $\Delta\lambda_F W/\xi^2$ must be resolved if one wants to separate the fermionic end states and the Majorana end

states. This is a stricter requirement than for energy levels in vortex cores, which are spaced by a distance $\sim \Delta(\lambda_F/\xi)$.²⁴ The distance ε_{\min} to the lowest-lying fermionic subgap excitation has a maximum for wire width $W \sim \xi$. The optimal value, $\varepsilon_{\min} \sim \Delta\lambda_F/\xi$, has the same scaling as in a vortex core.

While the end states obscure the identification of a topological phase through a density-of-states measurement, the presence of localized fermionic states near the wire ends does not necessarily inhibit topological quantum computation based on the Majorana states.^{26,40} In fact, the large gap $\sim \Delta$ to the delocalized bulk excitations makes the narrow limit $W/\xi \ll 1$ favorable for topological protection. On the other hand, the lateral Majorana modes are delocalized, and their presence at low energy for $W \gtrsim \xi$ poses a restriction on the use of the Majorana end states for topological quantum computation.

It is important to point out that the end states we discussed here exist at the ends of multichannel superconducting wires. The situation is different at an interface between two regions in which the channel numbers changes by a small amount only. This is the relevant scenario if for semiconductor-based topological superconductors, where the change in channel number is induced by a small change in a gate voltage. In that case the number of fermionic subgap states localized at the interface is at most half the difference in channel number. In particular, if the channel number changes by one, the interface harbors a Majorana fermion, but no low-lying fermionic states.

We close with a remark on the effect of disorder. Even weak disorder is known to lead to the formation of subgap states localized somewhere in the bulk of the superconductor, with an algebraic density-of-states low energy.^{17,41} The effect of weak disorder on the low-energy end states, in contrast, is expected to be small, because the disorder potential has vanishing matrix elements between the basis states (6) that are used for the construction of the effective end-state Hamiltonian (7). This is consistent with the findings of Refs. 19 and 20.

We gratefully acknowledge discussions with M. Duckheim, A. Romito, V. Lahtinen, G. Möller, S. Simon, Y. Oreg, and F. von Oppen. This work is supported by the Alexander von Humboldt Foundation.

¹F. Wilczek, *Nat. Phys.* **5**, 614 (2009).

²M. H. Freedman, *Proc. Natl. Acad. Sci. USA* **95**, 98 (1998).

³A. Kitaev, *Ann. Phys.* **303**, 2 (2003).

⁴A. Kitaev, *Ann. Phys.* **321**, 2 (2006).

⁵C. Nayak, S. H. Simon, A. Stern, M. Freedman, and S. Das Sarma, *Rev. Mod. Phys.* **80**, 1083 (2008).

⁶L. Fu and C. L. Kane, *Phys. Rev. Lett.* **100**, 096407 (2008).

⁷A. Cook and M. Franz, *Phys. Rev. B* **84**, 201105(R) (2011).

⁸M. Duckheim and P. W. Brouwer, *Phys. Rev. B* **83**, 054513 (2011).

⁹S. B. Chung, H.-J. Zhang, X.-L. Qi, and S.-C. Zhang, *Phys. Rev. B* **84**, 060510 (2011).

¹⁰H. Weng, G. Xu, H. Zhang, S. C. Zhang, X. Dai, and Z. Fang, *Phys. Rev. B* **84**, 060408 (2011).

¹¹Y. Oreg, G. Refael, and F. von Oppen, *Phys. Rev. Lett.* **105**, 177002 (2010).

¹²R. M. Lutchyn, J. D. Sau, and S. Das Sarma, *Phys. Rev. Lett.* **105**, 077001 (2010).

¹³J. Alicea, Y. Oreg, G. Refael, F. von Oppen, and M. P. A. Fisher, *Nat. Phys.* **7**, 412 (2011).

¹⁴R. Jackiw and C. Rebbi, *Phys. Rev. D* **13**, 3398 (1976).

¹⁵A. Y. Kitaev, *Phys. Usp.* **44**, 131 (2001).

¹⁶N. Read and D. Green, *Phys. Rev. B* **61**, 10267 (2000).

¹⁷O. Motrunich, K. Damle, and D. A. Huse, *Phys. Rev. B* **63**, 224204 (2001).

¹⁸M. Wimmer, A. R. Akhmerov, M. V. Medvedyeva, J. Tworzydło, and C. W. J. Beenakker, *Phys. Rev. Lett.* **105**, 046803 (2010).

¹⁹A. C. Potter and P. A. Lee, *Phys. Rev. Lett.* **105**, 227003 (2010).

²⁰R. M. Lutchyn, T. D. Stanescu, and S. Das Sarma, *Phys. Rev. Lett.* **106**, 127001 (2011).

- ²¹A. C. Potter and P. A. Lee, *Phys. Rev. B* **83**, 184520 (2011); **84**, 059906(E) (2011).
- ²²T. D. Stanescu, R. M. Lutchyn, and S. Das Sarma, *Phys. Rev. B* **84**, 144522 (2011).
- ²³B. Zhou and S.-Q. Shen, *Phys. Rev. B* **84**, 054532 (2011).
- ²⁴C. Caroli, P. G. De Gennes, and J. Matricon, *Phys. Lett.* **9**, 307 (1964).
- ²⁵N. B. Kopnin and M. M. Salomaa, *Phys. Rev. B* **44**, 9667 (1991).
- ²⁶A. R. Akhmerov, *Phys. Rev. B* **82**, 020509 (2010).
- ²⁷C. Gils, E. Ardonne, S. Trebst, A. W. W. Ludwig, M. Troyer, and Z. Wang, *Phys. Rev. Lett.* **103**, 070401 (2009).
- ²⁸A. W. W. Ludwig, D. Poilblanc, S. Trebst, and M. Troyer, *New J. Phys.* **13**, 045014 (2011).
- ²⁹K. G. Wilson, *Phys. Rev. D* **10**, 2445 (1974).
- ³⁰D.-H. Lee, G.-M. Zhang, and T. Xiang, *Phys. Rev. Lett.* **99**, 196805 (2007).
- ³¹N. Bray-Ali, L. Ding, and S. Haas, *Phys. Rev. B* **80**, 180504 (2009).
- ³²A. P. Schnyder, S. Ryu, A. Furusaki, and A. W. W. Ludwig, *Phys. Rev. B* **78**, 195125 (2008).
- ³³A. Kitaev, e-print [arXiv:0901.2686v2](https://arxiv.org/abs/0901.2686v2).
- ³⁴V. Lahtinen and J. K. Pachos, *Phys. Rev. B* **81**, 245132 (2010).
- ³⁵L. Mao, J. Shi, Q. Niu, and C. Zhang, *Phys. Rev. Lett.* **106**, 157003 (2011).
- ³⁶G. Kells, J. Kailasvuori, J. Slingerland, and J. Vala, *New J. Phys.* **13**, 095014 (2011).
- ³⁷See Supplemental Material at <http://link.aps.org/supplemental/10.1103/PhysRevB.85.060507> for a discussion of the lattice model and related material.
- ³⁸S. Tewari, S. Das Sarma, and Dung-Hai Lee, *Phys. Rev. Lett.* **99**, 037001 (2007).
- ³⁹R. S. K. Mong and V. Shivamoggi, *Phys. Rev. B* **83**, 125109 (2011).
- ⁴⁰G. Möller, N. R. Cooper, and V. Gurarie, *Phys. Rev. B* **83**, 014513 (2011).
- ⁴¹P. W. Brouwer, M. Duckheim, A. Romito, and F. von Oppen, *Phys. Rev. B* **84**, 144526 (2011).